CWE-8
June 7-11, 2026
London, ON, Canada

Buffeting-resistant design of bridge deck shape under synoptic and non-synoptic wind scenarios

Miguel Cid Montoya [a], Santiago Hernández [b]

[a] *Clemson University, Clemson, SC 29634, USA, mcidmon@clemson.edu*
[b] *University of La Coruña, La Coruña, Spain, hernandez@udc.es*

SUMMARY

This investigation addresses the buffeting-resistant design of wind-sensitive bridges under non-synoptic winds. The bridge displacements are assessed using a nonlinear time-domain buffeting analysis method that utilizes reduced viscoelastic models (RVEM) to transfer shape-dependent flutter derivatives and admittance functions from the frequency to the time domain. These parameters are predicted by an aeroelastic surrogate trained using forced vibration CFD simulations as a function of the deck shape, reduced velocity, and the mean angle of attack. To adapt this formulation to non-synoptic wind scenarios, the surrogate is recast as an aerodynamic transfer emulator, where the inputs are the deck shape and mean angle of attack, and the outputs are the RVEM´s stiffness, damping, and mass parameters. The methodology is conceived to be integrated into aero-structural optimization frameworks that simultaneously consider bridge responses under both synoptic and non-synoptic winds while accounting for the nonlinearities of shape-, angle of attack-, and frequency-dependent flutter derivatives.

Keywords: *Non-linear buffeting, Non-synoptic winds, Aero-structural optimization, Reduced viscoelastic models*

1. INTRODUCTION

Long-span bridges are affected by various wind scenarios throughout their lifespan. This may include non-synoptic winds, such as storms characterized by low-frequency variations of the deck mean angle of attack and relevant changes in the mean wind velocity (Fenerci and Oiseth, 2018; Barni et al., 2022; Calamelli et al., 2024). Consequently, aero-structural design and optimization frameworks (Cid Montoya et al., 2023) must be recast to consider the bridge wind-induced response under all possible wind conditions. This investigation explores the incorporation of buffeting-induced displacements into aero-structural optimization frameworks under non-synoptic wind scenarios, aiming to enhance the performance and safety of bridges during non-synoptic wind events. This requires the formulation of a parametrized nonlinear time-domain buffeting analysis that considers the impact of bridge design modifications on the buffeting analysis process.

2. NONLINEAR BUFFETING-DRIVEN AERO-STRUCTURAL DESIGN OF BRIDGES

2.1. Nonlinear buffeting analysis under non-synoptic winds

Following the band superposition concept, the buffeting response is computed as the addition of two components: (1) the low-frequency component and (2) the high-frequency component. The split between the two components can follow two different criteria: (1) aerodynamics, as proposed by Calamelli et al. (2024) or (2) structural dynamics, as proposed by Chen and Kareem (2001) and Barni et al. (2022). In the current investigation, we define three cut-off frequencies ($f_{cut,L}$, $f_{cut,V}$, $f_{cut,T}$) as a function of the bridge dynamic characteristics:

$$f_{cut,L} = f_{L1}(\mathbf{x});\ f_{cut,V} = f_{V1}(\mathbf{x});\ f_{cut,T} = f_{T1}(\mathbf{x}) \tag{1}$$

where **x** is a vector with all the design variables used in the aero-structural optimization, such as deck shape and size, cables definition, etc., that impact the natural frequencies. f_{L1}, f_{V1}, and f_{T1} are the first lateral, vertical, and torsional frequencies. Hence, both the low- and high-frequency components are impacted by the deck shape and other design variables via the cut-off frequencies, such as the mean angle of attack, which modulates the self-excited and buffeting forces.

2.2. High-frequency component formulation via reduced viscoelastic models (RVEM).

Similar to Calamelli et al. (2024), we model the aeroelastic forces using dynamic systems. However, we formulate the viscoelastic models in their "reduced form", defined as Reduced Viscoelastic Models (RVEM), so that the aerodynamic transfers are independent of the mean wind velocity U_m. As an example, a serial Kelvin-Voigt-Mass system composed of a mass, two springs and two dampers, can be modeled for the vertical self-excited force $F_z(t)$ in the time domain as

$$F_z = k_1 z(t) + \frac{Br_1}{2\pi U_m}\dot{z}(t) - k_1\mu(t) - \frac{Br_1}{2\pi U_m}\dot{\mu}(t) \tag{2}$$

$$m^2\left(\frac{B}{2\pi U_m}\right)^2 + (r_1 + r_2)\frac{B}{2\pi U_m}\dot{\mu}(t) + (k_1 + k_2)\mu(t) = \frac{Br_1}{2\pi U_m}\dot{z}(t) + k_1 z(t) \tag{3}$$

Aiming at avoiding the dependency on U_m, which is an important issue when dealing with non-synoptic wind scenarios, as the mean velocity presents relevant slow variations with time, the Fourier transform of Eqs. (2) and (3) were made using the reduced velocity U^*, leading to

$$TF_z = \frac{B}{2\pi U_m}\left[\frac{\left(\frac{ir_1}{U^*}+k_1\right)\left(\frac{-m}{U^{*2}}+\frac{ir_2}{U^*}+k_2\right)}{\frac{-m}{U^{*2}}+\frac{i(r_1+r_2)}{U^*}+(k_1+k_2)}\right]\hat{z}(U^*) \tag{4}$$

Eq (4) is only a function of the U^*, hence, the RVEM are independent of the mean wind velocity U_m. The methodology was validated in the context of the ongoing IABSE TG.3.1 (Diana et al. 2025) against experimental measurements of the Hardanger Bridge.

2.3. From aeroelastic surrogates to aerodynamic transfer emulators

Linear time-domain aeroelasticity methods require the emulation of the force coefficients (C_D, C_L, C_M), flutter derivatives (A_i^*, H_i^*, P_i^*) and admittance functions $(\chi_{Du}^*, \chi_{Lu}^*, \chi_{Mu}^*, \chi_{Dw}^*, \chi_{Lw}^*, \chi_{Mw}^*)$ as a function of the deck shape S_d, mean angle of attack α_m, and reduced velocity U^* to properly conduct the buffeting-resistant design (Verma et al., 2025):

$$\mathcal{A}(S_d, \alpha_m, U^*) = [C_D, C_L, C_M, A_i^*, H_i^*, P_i^*, \chi_{Du}^*, \chi_{Lu}^*, \chi_{Mu}^*, \chi_{Dw}^*, \chi_{Lw}^*, \chi_{Mw}^*] \tag{5}$$

However, non-linear buffeting analysis based on RVEM requires modulating the stiffness $k_{k,j}^i$, damping $r_{k,j}^i$, and mass $m_{k,j}^i$ parameters, which are defined based on the surrogate model provided in Eq. (5), as a function of the deck shape S_d, and mean angle of attack α_m. Hence, a new surrogate model, the aerodynamic transfer emulator $\mathcal{E}_{RVEM}$, can be defined as a function of S_d and α_m as:

$$\mathcal{E}_{RVEM}(S_d, \alpha_m) = \left[m_{k,j}^i, r_{k,j}^i, k_{k,j}^i\right], \tag{6}$$

Where subindex k stands for the aeroelastic matrix component, being k=1,..9, j refers to the number of RVEM among those combined in the transfer function, and i is the index of the parameter.

3. CASE STUDY: A BLUFF SINGLE-BOX DECK WITH VARIABLE DEPTH

A long-span bridge equipped with a bluff deck cross-section, based on the Sunshine Skyway Bridge, will be used as a case study. The deck depth is considered a design variable that can be changed by ±43.5% with regard to the baseline geometry, as shown in Figure 1 (a). Figure 1 (b) shows the velocity flow fields at the maximum amplitude instant ($\alpha\,(t) = +2°$) of the pitching forced vibration at reduced velocity $U^* = 6.5$ for three deck geometries: the baseline geometry (H/B = 0.1556), and the lower and upper bounds of the design domain, i.e., H/B = 0.1104 and H/B = 0.2232, respectively. A kriging surrogate model was build using information from 432 CFD simulations, including six geometries (H/B = [0.1104, 0.1330, 0.1556, 0.1781, 0.2007, 0.2232]), six reduced velocities ($U^* = [3.0, 5.0, 6.5, 10.0, 15.0, 20.0]$), four mean angles of attack ($\alpha_m = [-2°, 0°, +2°, +4°]$), and three degrees of freedom (pitching, heaving, and shoving). Extensive verification studies were conducted in Verma et al. (2024, 2025). The 18 flutter derivatives obtained for each sample (H/B, U^*, α_m) will be used to fit the RVEM defined in Section 2.2. and train aerodynamic transfer emulators (Eq. 5). It is worth noting that this bluff deck cross-section exhibits a very interesting aeroelastic behavior. As discussed in Verma et al. (2025), the sign of A_2^* changes as the mean angle of attack increases, with this pattern being more prominent for bluff geometries. Moreover, the mean angle of attack at which the A_2^* sign flip happens decreases with the level of bluffness. This feature will be reflected in the torsional buffeting response of the bridge.

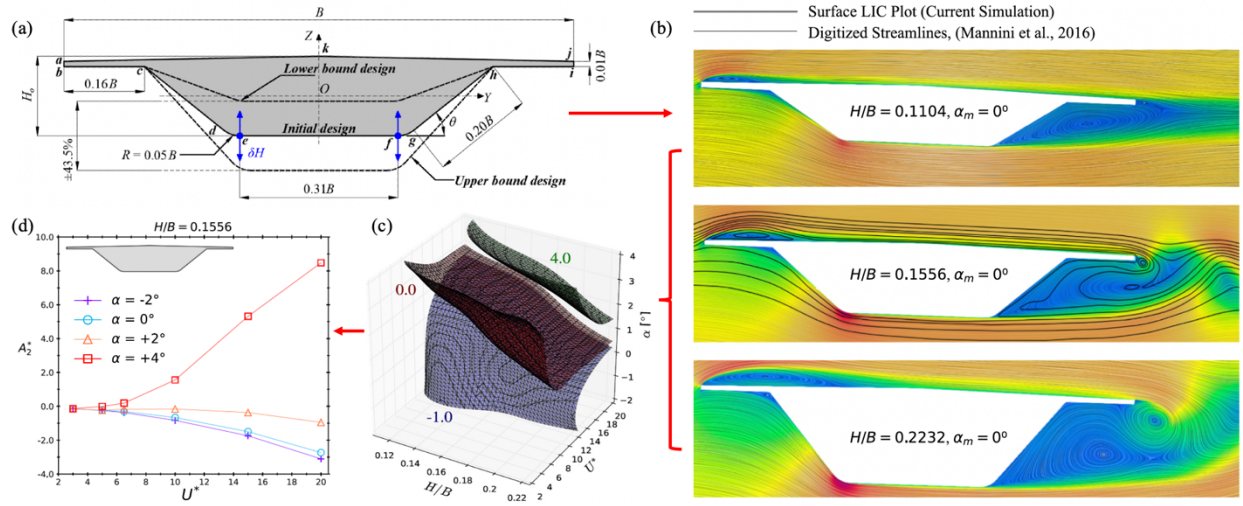

Figure 1: Aeroelastic response of the deck with variable depth: (a) Deck cross-section geometry and shape design domain; (b) Flow fields of three deck shapes including the baseline design and the lower and upper bounds of the design domain at $\alpha_m = 0°$ and $\alpha\,(t) = +2°$; (c) response isosurface of the aeroelastic surrogate for flutter derivative A_2^*; and (d) sensitivity of A_2^* with α_m for H/B=0.1556 showing the sign change between $\alpha_m = +2°$ and $+4°$.

4. PRELIMINARY RESULTS AND CONCLUDING REMARKS

Figure 2 (a) shows the horizontal component of the wind time series compared to the low frequency components after being filtered with three cut-off frequencies (see Eq. 1). Subplot (b) shows a detail of the gust, and subplots (c) and (d) show the high frequency component. The wind time series is the TH-B used by the IABSE TG3.1. (Diana et al. 2025), based on the data reported by Fenerci and Oiseth (2018). Subplots (e) and (f) show the high-frequency component of the lateral response of the bridge for deck shapes H/B = 0.1556 and H/B = 0.2232. The impact of the deck bluffness on the bridge response is clear, as the lateral displacements have been tripled by

increasing the deck depth due to its impact on its aeroelastic parameters. Extended and detailed results will be presented in the oral presentation.

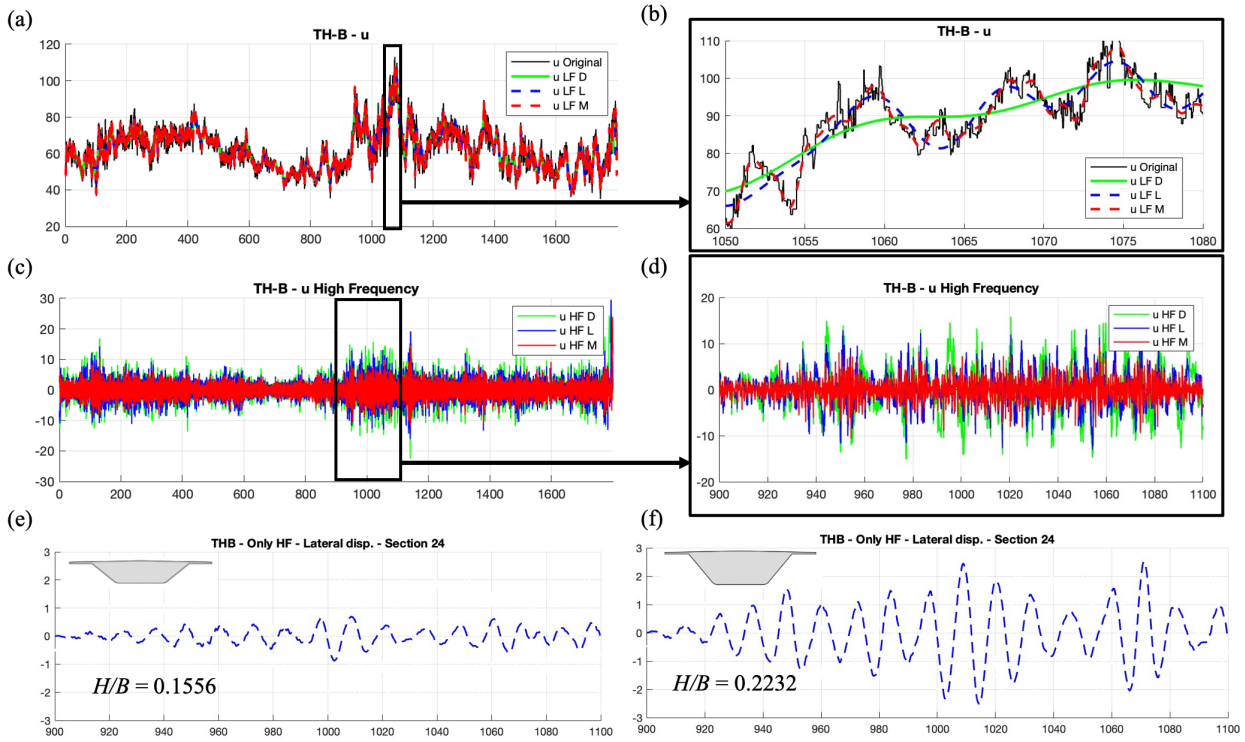

Figure 2: Wind time series (a-d) and buffeting-induced lateral displ. for H/B=0.1556 (e) and H/B=0.2232 (f).

ACKNOWLEDGEMENTS

The authors thank the National Science Foundation (CMMI-2503131) and Xunta de Galicia (ED431C 2025/35).

REFERENCES

Barni, N., Oiseth, O., & Mannini, C. (2022). Buffeting response of a suspension bridge based on the 2D rational function approximation model for self-excited forces. Engineering Structures, 261, 114267.

Calamelli, F., Rossi, R., Argentini, T., Rocchi, D., & Diana, G. (2024). A nonlinear approach for the simulation of the buffeting response of long span bridges under non-synoptic storm winds. J. Wind Eng. Ind. Aerodyn., 247, 105681.

Chen, X., & Kareem, A. (2001). Nonlinear response analysis of long-span bridges under turbulent winds. J. Wind Eng. Ind. Aerodyn., 89, 1335–1350.

Cid Montoya, M., Hernández, S., & Kareem, A. (2022). Aero-structural optimization-based tailoring of bridge deck geometry. Engineering Structures, 270, 114067.

Diana, G., Stoyanoff, S., Argentini, T., Barni, N., Calamelli, F., Cid Montoya, M., Hernández, S., Larsen, A., Mannini, C., Rocchi, D., Rossi, R., Svendsen, M., Wu, T. (2025). IABSE TG3.1 final analysis: Comparison between full-scale measurements and numerical simulations of a long-span bridge during a non-synoptic event. IABSE Congress Ghent 2025.

Fenerci A., Øiseth O. (2018) Strong wind characteristics and dynamic response of a long-span suspension bridge during a storm. Journal of Wind Engineering and Industrial Aerodynamics; 172, 116–138.

Verma, S., Cid Montoya, M., & Mishra, A. (2024). Shape- and frequency-dependent self-excited forces emulation for the aero-structural design of bluff deck bridges. J. Wind Eng. Ind. Aerodyn., 252, 105769.

Verma, S., Cid Montoya, M., & Mishra, A. (2025). Aero-structural design of bridge decks under synoptic and non-synoptic winds via aeroelastic surrogates comprising shape, reduced velocity, and mean angle of attack. J. Wind Eng. Ind. Aerodyn., 265, 106133.